Condition Assessment of Metal Oxide Surge Arrester Based on Multi-Layer SVM Classifier

M. Khodsuz* and M. Mirzaie*(C.A.)

Abstract: This paper introduces the indicators for surge arrester condition assessment based on the leakage current analysis. Maximum amplitude of fundamental harmonic of the resistive leakage current, maximum amplitude of third harmonic of the resistive leakage current and maximum amplitude of fundamental harmonic of the capacitive leakage current were used as indicators for surge arrester condition monitoring. Also, the effects of operating voltage fluctuation, third harmonic of voltage, overvoltage and surge arrester aging on these indicators were studied. Then, obtained data are applied to the multi-layer support vector machine for recognizing of surge arrester conditions. Obtained results show that introduced indicators have the high ability for evaluation of surge arrester conditions.

Keywords: Condition Monitoring, Indicator, Leakage Current, Metal Oxide Surge Arrester, Multi-Layer Support Vector Machine.

1 Introduction

The reliable and enough energy is an essential requirement of customers which must be supplied by electrical power system. This requirement should be supplied by electrical power system at all functional levels of production, transmission and distribution of electrical energy. According to the most recent studies, equipment monitoring is the best application method for the increase of reliability and equipments failure diagnostic [1-3].

Metal Oxide Surge Arresters (MOSAs) are one of the most important equipments applied in power system for protection against switching and lightning over-voltages. Surge arresters failures can damage to other substation equipment.. Thus, they positively contribute to increase reliability and performance of the power system and their condition monitoring has significant influence on the reliability of power system. MOSAs characteristics during utilization vary due to the several factors, of which the most important factors are: aging due to operating voltage and impulse current, penetration of moisture into the housing and chemical reaction with the surrounding atmosphere. Degradation of metal oxide surge arresters due to these destructive factors leads to increase leakage currents [4-7]. Online and offline methods can be performed for leakage current measurement which accurate results may be obtained by using offline methods. The requirement of expensive equipment and surge arrester disconnecting from the system are drawbacks of offline method. The most common methods for evaluation of metal oxide surge arrester condition are online methods. Leakage current measurement method under voltage system [8-12], temperature measurement [13-14] and electro-magnetic field measurement [15-16] are online methods that are used for metal oxide surge arrester monitoring.

The majority of most methods in literatures are based on surge arrester leakage current at operating voltage, which is based on harmonic analysis of the total leakage current, the third order harmonic of the resistive leakage current, power loss measurement and resistive leakage current amplitude measurement [8-11].

Ref. [17] has introduced the fundamental frequency of the resistive leakage current as more accurate indicator than proposed indicators in [8-11] for surge arrester condition monitoring. But, according to the obtained results in this paper, this indicator can't diagnose various conditions of surge arresters. Therefore other indicators should be used to improve condition monitoring.

This paper investigates good indicators for surge arrester condition based on leakage current analysis. Maximum amplitude of resistive fundamental harmonic (I_{mr1}), Maximum amplitude of resistive third harmonic (I_{mr3}) and maximum amplitude of capacitive fundamental harmonic (I_{mc1}) have been used for surge arrester condition monitoring [18].

In this work, all calculations and analysis were

Iranian Journal of Electrical & Electronic Engineering, 2015.
Paper first received 07 Jun. 2015 and in revised form 27 Sep. 2015.
* The Authors are with the Department of Electrical and Computer Engineering, Babol University of Technology, Babol, Iran.
E-mails: m.khodsoz@stu.nit.ac.ir and mirzaie@nit.ac.ir.

performed using MATLAB, ATP-EMTP and MAXWELL computing software. Medium voltage surge arrester was used to study operating voltage fluctuation, voltage third harmonic, overvoltage and aging effects. In this paper to show the applicability of indicators Multi-Layer Support Vector Machine (MLSVM) was used for classification and recognition task. This tool is able to distinguish above conditions based on features information with acceptable precision. This is the novelty of paper which has not been considered ago.

2 Medium Voltage Surge Arrester Modeling

Metal oxide surge arresters have nonlinear voltage-current characteristic that this characteristic can be divided to two regions. In the first region, voltage is lower than nominal voltage and small leakage current flows through surge arresters. In second region, very small voltage changes correspond to exceptionally large changes of current. In the third region, not only voltage is higher than residual voltage but also current is bigger than rated current.

Under normal operating conditions, a small leakage current flow through surge arresters to ground that corresponds to the first section of surge arresters V-I characteristic. Surge arrester leakage current under steady-state conditions consists of capacitive and resistive components. Capacitive component of total leakage current appears under the fundamental frequency of the applied voltage and the resistive component is a non-sinusoidal waveform consists of the fundamental frequency component and odd harmonics components. Fig. 1 shows surge arrester equivalent circuit to investigate surge arrester leakage current in 20 kV network [18]. Also, Table 1 shows the surge arrester characteristics.

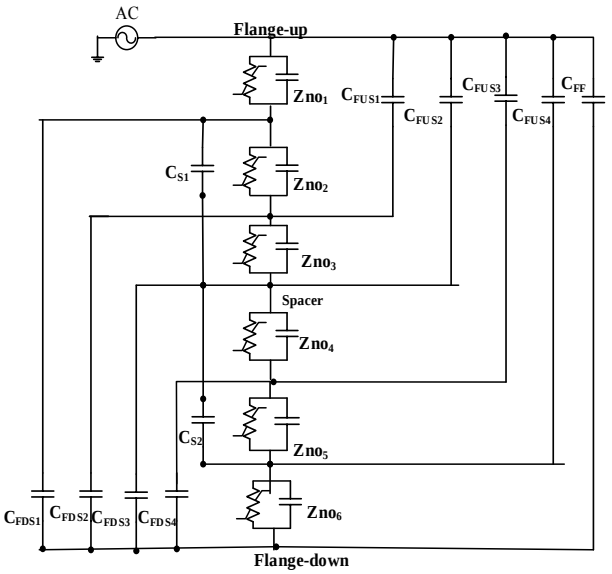

Fig. 1 Medium voltage surge arrester equivalent circuit.

Table 1 Technical characteristics of studied surge arresters.

Surge Arrester Type	
Rated voltage (kV)	25
Continuous operating voltage (kV)	20
lightning impulse current with 8/20 μs (kA)	10
Maximum residual voltage (kV)	70
Total external creepage distance (mm)	800
Shed numbers	8
Varistor numbers	6

In Fig. 1, C_{FF} is Capacitance between upper and lower flanges, C_{FUSi} (i=1, 2…4) are stray capacitances of upper flange with spacer and aluminums sheets, C_{FDSi} (i=1, 2… 4) are stray capacitances of lower flange with spacer and aluminums sheets and C_{Si} (i=1, 2) are capacitances between spacer and aluminum sheets.

Fig. 2 shows the typically obtained applied voltage waveform U(t) and total leakage current. Total measured leakage current (i_t) consists of capacitive (i_c) and resistive (i_r) components.

As shown in Fig. 2, divided resistive have fundamental and higher order harmonics. The creation of higher order harmonics in resistive current are caused by the varistor non-linearity behavior. Due to the pure sinusoid applied voltage, capacitive component has only fundamental component.

3 Voltage Fluctuation Influence

In order to study the influence of voltage fluctuation, surge arrester model as shown in Fig. 1 was used. The normal operating voltage was simulated by a pure cosine function with 1pu amplitude (U_m=1 pu). For the simulation of voltage fluctuation, the operating voltage was varied in the range 0.95 U_m to 1.05 U_m.

The measured total leakage current consists of resistive and capacitive components. In this work, the time-delay addition method [19] is used to extract resistive component. This method is able to separate the resistive current and capacitive current components from the total leakage current without measuring the voltage across the surge arrester.

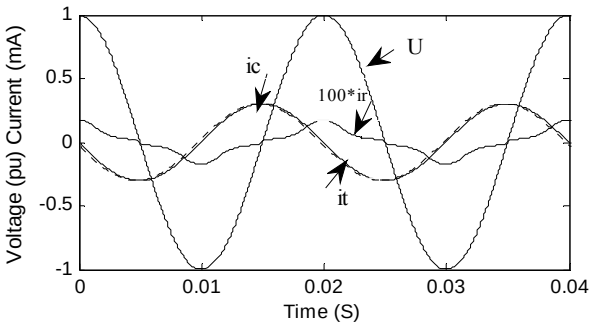

Fig. 2 Typical waveforms of metal oxide surge arrester voltage and current.

The harmonic analysis of obtained current signals is done by employing the FFT algorithm in MATLAB software. Table 2 shows the values of indicators under applied voltages U_m, 0.95 U_m and 1.05 U_m.

According to the results as shown in Table 2, indicator I_{mr1} under voltage U_m has the value of 0.896 μA and under voltage 0.95 U_m is 0.753 μA that shows a decrease of 15.9%. At voltage 1.05 U_m, I_{mr1} increases to 1.0895 μA which it is almost 21.6% greater than its value at nominal operating voltage U_m. In comparison with its value under nominal voltage U_m, the variation of under 0.95 U_m and 1.05 U_m, is -27.4% and 41.98%, respectively.

When the applied voltage is 105% Um, I_{mc1} has the value of 221.64 μA. The increase of I_{mc1} in this applied voltage is 5% in comparison with its value at voltage U_m. In comparison with its value at nominal voltage U_m, I_{mc1} shows a diminishing of 5% at 95% U_m. It can be concluded that the variation of this indicator is proportional to the surge arrester voltage fluctuation and can be used for evaluating the surge arrester condition. Therefore by measuring this indicator and compared with fundamental harmonic of capacitive component at nominal operating voltage, it can be realized the voltage fluctuation at leakage current measurement moment.

4 The Influence of Overvoltage

Overvoltage in power systems may be generated by external and internal events, such as lightning, switching, load rejection, etc. In a case that surge arrester is stressed with overvoltage during its leakage current measurement, the measured leakage current consists of measurement error. Therefore, the amplitudes of capacitive and resistive components are greater than their values at normal operation voltage. Consequently, to realize overvoltage at current measurement instant and to prevent the incorrect diagnosis of surge arrester condition, the voltage across surge arrester must be measured.

In this paper, the overvoltage, occurred during current measurement, was realized through new introduced indicator (I_{mc1}) without voltage measuring. To study the influence of overvoltage, the applied voltage of surge arrester was changed in the range of 1.05 to 1.25Um and then leakage current was measured.

Table 3 shows the influence of overvoltage on the values of introduced indicators. According to the results as shown in Table 2, the increase of overvoltage amplitude causes the increments of indicators I_{mr1} and I_{mr3}.

The magnitude of overvoltage during current measurement could be calculated as follow:

$$overvoltage\ amplitude = \frac{I_{mc1(measured)}}{I_{mc1(Um)}} * Um \quad (1)$$

According to the Eq. (1), the increase of the value of indicator I_{mc1} is proportional to the overvoltage magnitude and the ratio of capacitive component under overvoltage condition to capacitive component in normal condition is a good criterion for identification of the existence of overvoltage during surge arrester current measurement.

It can be concluded that, the best result is provided by the indicator I_{mc1} to detect overvoltage during current measuring and it is the most sensitive to network voltage variations.

5 The Influence of Voltage Harmonics

In this section, the capability of proposed indicators under the presence of operating voltage harmonics has been analyzed. The allowable values of harmonics of voltage depending on the voltage level where the maximum acceptable value of the third harmonic of voltage is 5% in LV–MV networks.

Under sinusoid applied voltage, the measured leakage current consists of resistive and capacitive components. Capacitive current has only fundamental harmonic. Suppose the applied voltage contains n^{th} harmonic component [20, 21]:

$$U(t) = U_1 \cos(\omega t) + U_n \cos(n\omega t + \theta_n) \quad (2)$$

where U_n is the maximum value of the n^{th} harmonic of voltage, ω is radial frequency of the fundamental harmonic, n is order of the harmonic, t is time, and θ_n is the initial phase of the nth harmonic.

Due to the existence of harmonic in applied voltage, capacitive current consists of fundamental and nth harmonic components:

$$i_c(t) = i_{c1}(t) + i_{cn}(t) \quad (3)$$

Resistive current includes of fundamental and other harmonic components:

$$i_{r1} = i'_{r1} + i''_{r1}$$
$$i_{rn} = i'_{rn} + i''_{rn} \quad (4)$$

where i'_{r1} and i'_{rn} are fundamental and n^{th} harmonics of resistive current respectively, which are the consequence of metal oxide surge arrester nonlinear characteristic. i''_{r1} and i''_{rn} are fundamental and n-th harmonics of resistive current respectively. These are the consequence of the existence of the higher harmonics in voltage.

Table 2 Values of indicators at different voltages level.

Indicator	95% U_m	U_m	105%U_m
I_{mr1}(μA)	0.753	0.896	1.0895
I_{mr3}(μA)	0.177	0.244	0.34644
I_{mc1}(μA)	200.31	211.04	221.64

Table 3 Values of indicators under network overvoltage.

Indicator	U_m	1.1U_m	1.15U_m	1.2U_m	1.25U_m
I_{mr1} (μA)	0.896	1.3591	1.7203	2.316	3.33
I_{mr3} (μA)	0.244	0.50322	0.713	1.112	1.84
I_{mc1} (μA)	211.04	232.143	242.7	253.2	263.8

5.1 The Influence of the Third Harmonic of Voltage

When the applied voltage includes 3th harmonic component, capacitive current consists of fundamental and third harmonic components. Measuring the amplitude and phase angle of the 3th harmonic of voltage is required to extract the third harmonic of capacitive current [11]. The introduced method in [18] is able to extract proper resistive and capacitive currents from total measured leakage current in pure sinusoid voltage without measuring the voltage across the surge arrester.

Consider the case, when the applied voltage isn't measured during leakage current measurement and it is supposed to be pure sinusoidal wave. In this case, when the method introduced in [19] is applied, the third harmonic of capacitive current insert to the third harmonic of resistive current and thus extracted capacitive current consists of only fundamental component. Therefore the third order harmonic of resistive current becomes greater than fundamental component and it can be used as a sign for identifying the existence of voltage harmonic during surge arrester current measurement.

Table 4 shows harmonic components of resistive and capacitive currents that extracted by introduced method in [19] and [11] for U_3=1%, θ_3=0. Every two methods have identical results except for I_{mr3} and I_{mc3}. Method [19] is based on pure sinusoid voltage and don't produce I_{mc3}, so third harmonic of capacitive current insert to the third harmonic of resistive current. Consequently, the third harmonic of resistive current is greater than the fundamental harmonic of resistive current. The amplitude of the third harmonic of voltage is obtained as follows:

$$U_3 = I_{mr3} / 3 I_{mc1} \quad (5)$$

Figs. 3–5 show the dependency of the introduced indicators (obtained from method [18]) on the third harmonic of voltage U_3 and the initial phase of the third harmonic θ_3. The third harmonic of voltage U_3 is within an interval of 0–5% and the initial phase of the third harmonic θ_3 is varied from -180° to 180°.

Third and fundamental harmonics of resistive current in pure sinusoid voltage show that the third harmonic of resistive current (I_{mr3}) is greater than fundamental harmonic (I_{mr1}).

Table 4 Harmonic components of resistive and capacitive currents (U_3=1%, θ_3=0).

Indicator	[11] |Method	[18] Method
I_{mr1}(μA)	0.978	0.978
I_{mr3}(μA)	0.264	6.3368
I_{mc1}(μA)	211.04	211.04
I_{mc3}(μA)	6.33	0

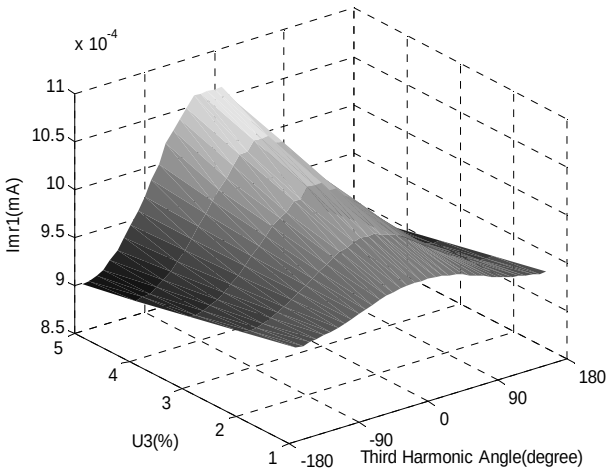

Fig. 3 Dependency of the I_{mr1} on the third harmonic of voltage U_3 and the initial phase of the third harmonic θ_3.

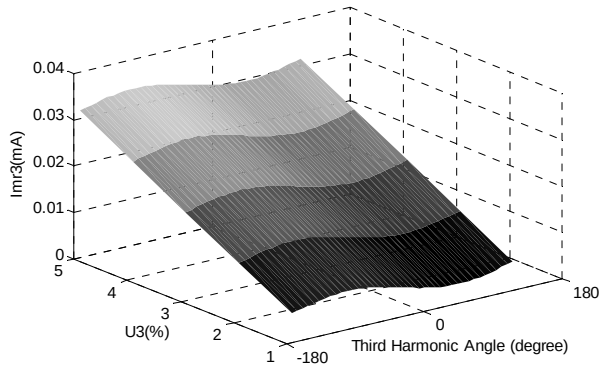

Fig. 4 Dependency of the I_{mr3} on the third harmonic of voltage U_3 and the initial phase of the third harmonic θ_3.

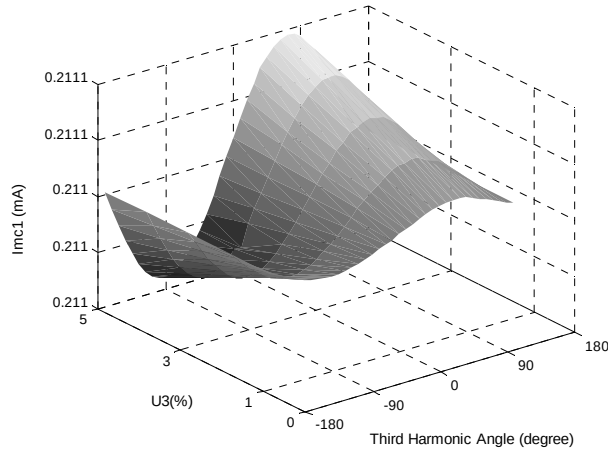

Fig. 5 Dependency of the I_{mc1} on the third harmonic of voltage U_3 and the initial phase of the third harmonic θ_3.

Also the third harmonic of voltage has the most effect on the third harmonic of resistive current indicator (I_{mr3}) while I_{mc1} is the least sensitive to the presence of third harmonic of voltage. This condition can be used as a feature for realizing the existence of voltage harmonic.

Based on above- mentioned facts, it can be seen that the amplitude of third harmonic and its initial phase has some influences on indicators. The maximum values of indicators I_{mc1} and I_{mr3} take place at $\theta_3 = 90°$ and $\theta_3 = -90°$, respectively. The maximum value for indicator I_{mr1} occurs at around $\theta_3 = 0°$.

6 The Influence of Aging

Metal oxide surge arresters can be degraded during utilization due to the destructive factors. Degradation of metal oxide surge arresters caused by destructive factors can damage them and thus change surge arresters U-I characteristic. Therefore, U-I characteristics of Zno blocks (was used in Fig. 1) was intentionally decreased to study aging effect. Ultimately, this condition was distinguished by introduced indicators. Normal voltage with a magnitude of U_m was applied to aged surge arrester to investigate the influence of aging on introduced indicators for each surge arrester block and complete aged surge arrester (total six blocks were aged). Table 5 and Table 6 show aging effect on introduced indicators for 15% and 20% reductions in U-I characteristic. According to these tables, it is clear that I_{mr1} and I_{mr3} in aged metal oxide surge arrester have greater values when compared to the corresponding values in un-aged surge arrester while I_{mc1} has a little change. So the observation and comparison of such variation in these indicators with their values in normal operating condition can be used for realizing aged surge arresters or aged Zno block in surge arrester. By comparing these tables with Table 3, it is obvious that all indicators I_{mr1}, I_{mr3} and I_{mc1} in overvoltage condition are greater than corresponding values in normal operation condition. Thus, the introduced indicators can be able to distinguish the overvoltage condition from aging condition correctly.

7 Multi-Layer Support Vector Machine

In this section, multi-layer SVM is used to recognize surge arrester conditions.

7.1 Review of SVM

Support vector machine was introduced by Vapnik and co-workers in the late 1990s. While traditional statistical theory keeps to Empirical Risk Minimization (ERM), SVM satisfies structural risk minimization (SRM) based on Statistical Learning Theory (SLT), whose decision rule could still obtain small error to independent test sampling. SVM mainly has two classes of applications, classification and regression. The classification problem can be restricted to consideration of the two-class problem without loss of generality. In this problem, the goal is to separate the two classes by a function (a classifier), which is induced from available examples and work well on unseen examples. There are many possible linear classifiers that can separate the data, but there is only one that maximizes the margin (maximizes the distance between it and the nearest data point of each class).

This linear classifier is termed the optimal separating hyperplane. In most instances, problems could not be separated linearly. Nonlinear classification algorithm is reviewed in this section [22, 23].

Given a set of training data:

$$D = \{(x_1, y_1),.., (x_i, y_i),.. , (x_l, y_l)\}, x \in R^n, y \in \{-1, 1\} \quad (6)$$

where xi is the training data, l the number of training data and y_i is the class label (1 or -1) for x_i.

Firstly, a nonlinear function is employed to map the original input space R^n to N-dimensional feature space:

$$\phi(x) = (\phi_1(x), \phi_2(x), \dots , \phi_N(x)) \quad (7)$$

Table 5 The influence of aging on surge arrester operation and introduced indicators (15% reduction).

Indicator	Un-Aged	Aged						
	U_m	First Block	Second Block	Third Block	Four Block	Five Block	Six Block	Total Block Aged
I_{mr1} (μA)	0.896	1.17	1.11	1.08	1.056	1.042	1.04	2.0036
I_{mr3} (μA)	0.244	0.415	0.369	0.348	0.33	0.325	0.324	0.89
I_{mc1} (μA)	211.04	211.0446	211.043	211.0426	211.0421	211.042	211.042	211.0425

Table 6 The influence of aging on surge arrester operation and introduced indicators (20% reduction).

Indicator	Un-Aged	Aged						
	U_m	First Block	Second Block	Third Block	Four Block	Five Block	Six Block	Total Block Aged
I_{mr1}(μA)	0.896	1.48	1.38	1.33	1.24	1.21	1.2	3.357
I_{mr3}(μA)	0.244	0.632	0.56	0.526	0.465	0.438	0.435	1.843
I_{mc1}(μA)	211.04	211.055	211.051	211.049	211.046	211.045	211.045	211.045

Then the separating hyperplane is constructed in this high dimension feature space. The classifier takes the form as:

$$y(x) = \text{sign}(w \cdot \phi(x) + b) \quad (8)$$

where w is the weight vector and b is a scalar.

To obtain the optimal classifier, $\|w\|$ should be minimized under the following constraints

$$y_i\,[\phi(xi)\cdot w + b] \geq 1 - \xi_i, \quad i = 1, 2, \ldots, l \quad (9)$$

The variables ξ_i are positive slack variables, which is necessary to allow misclassification.

Thus, according to principle of structural risk minimization, the optimal problem can be formulated as minimization of the following objective function J:

$$\begin{aligned} &Min\ j(\mathrm{w},\xi) = \frac{1}{2}\|w\|^2 + C\Sigma_{i=1}^{l}\xi \\ &Subject\ to\ y_i[\phi(xi)\cdot w + b] \geq 1 - \xi_i \quad \xi_i \geq 0, i = 1, \ldots, l \end{aligned} \quad (10)$$

where C is the margin parameter and controls the tradeoff between errors of the SVM on training data and margin maximization.

SVM is able to separate two classes by a classifier. Due to this limitation, multi-Layer SVM is used to classify more than two classes. Fig. 6 shows multi-Layer SVM structure that classifies three classes. The first SVM (SVM1) is trained to separate class1 from other classes and the second SVM (SVM_2) separates class 2 and class 3 from each other. Because of special training data for every SVM, it is not able to change SVMs location after training process. Generally n-1 SVMs is required to classify n classes from each other.

If the first SVM fails to correctly classify the samples, some samples of the class1 are passed to the next layer. In this case, these shifted samples categorize by SVM2 in class 2 or class 3. So the accuracy rate of classifier decreases. This is the most disadvantage point of this structure. To solve this problem, n SVMs for the classification of n classes are required. Therefore, samples that have not been classified in this structure of multi-layer SVM, transfer to the last layer and compose non-classification class.

7.2 Classification Results

In this section, the ability of new indicators via Multi-Layer SVM has been evaluated. For this purpose a dataset for different conditions of surge arresters have been used which 60% of data have been used for training of the classifier and the rest for testing. Fig. 7 shows data dispersion which obtained from simulation.

According to Fig. 7, Imr_1 criterion is in good agreement with the samples' ageing and overvoltage condition. These two conditions can be separated from other classes with this criterion. Also Imc_1 can be used to only distinguish aged condition from overvoltage. To separate harmonic samples from voltage fluctuation ones, Imr3 can be used as effective indicator and it has to be used for recognizing this class. Figs. 8 and 9 show the basic principle of training and testing of multi-layer SVM classifier, respectively. All of the four SVMs of the classifier adopt Gaussian radial basis function as their kernel. Based on the characteristics of different surge arrester conditions, four SVMs are developed to identify the four aforementioned conditions. SVM1 is established to train the first layer classification. SVM1 classify the harmonic condition class and other classes.

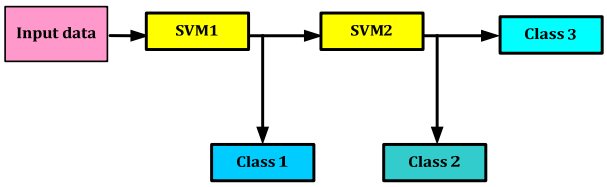

Fig. 6 Multi- layer Support Vector Machine structure.

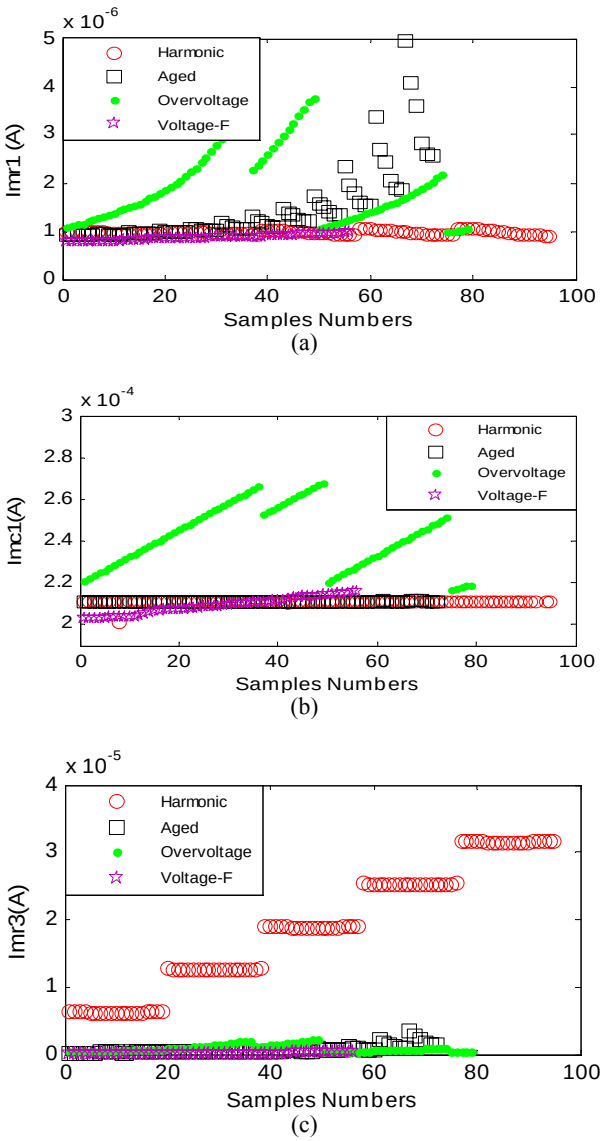

Fig. 7 The dispersion of samples.

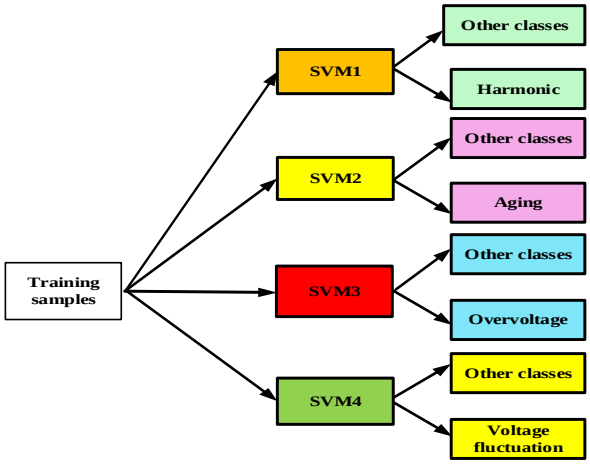

Fig. 8 The principle of Multi-Layer SVM training.

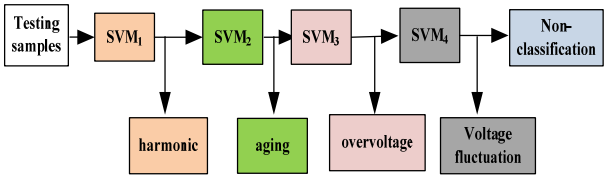

Fig. 9 The schematic of surge arrester condition diagnosis based on Multi-Layer SVM.

If the class is harmonic condition, the output of SVM_1 is -1; otherwise the output is +1. The second SVM (SVM_2) is trained to separate aged state from two other states. SVM_3 is established to train the third layer classification and distinguish overvoltage from voltage fluctuation condition and finally SVM_4 trains to segregate voltage fluctuation state from non-classification samples.

After training the network, the testing samples are inputted into the trained Multi-layer SVMs. According to the output, the four classes can be classified. Table 7 shows the details of samples that used for training and testing of Multi-Layer SVM.

Table 8 shows the accuracy of Multi-Layer SVM classifier. According to the tables, it is clear that the classification accuracy rate for every SVM in this classifier is in a good criterion. Also obtained results show that the Multi-Layer SVM classifier has a good performance and is able to distinguish surge arrester different conditions. On the other hand, the excellent performance of the classifier shows the high applicability of proposed indicators for correct diagnostic of arrester's condition.

Table 7 The details of Multi-layer SVM classifier performance

Classification Type	Multi-Layer SVM Classifier Results					Samples Numbers	
	Non-Classification	Voltage Fluctuation	Overvoltage	Aging	Harmonic	Test	Train
Harmonic	1	0	0	0	39	40	55
Aging	1	0	0	26	0	27	45
Overvoltage	0	0	30	0	0	30	49
Voltage fluctuation	0	23	1	0	0	24	32
Sum	2	23	31	26	39	121	181

Table 8 The accuracy of Multi-Layer SVM.

	Input	Correct	Incorrect	Accuracy %
SVM_1	121	120	1	99.17
SVM_2	82	81	1	98.78
SVM_3	56	56	0	100
SVM_4	26	25	1	96.15
Multi-Layer SVM	121	118	3	97.52

8 Conclusion

In view of the analysis of the calculation results, the following conclusions can be made:

- The influence of voltage fluctuation on the applicability of the introduced indicator is obvious. In the case of voltage fluctuation, all introduced indicators change but the best indicator for evaluating the surge arrester condition is the fundamental harmonic of capacitive leakage current I_{mc1}. So by measuring this indicator and comparing it with its value at nominal operating voltage, we can realize voltage fluctuation at leakage current measurement time.
- The existence of overvoltage during leakage current measuring causes the increase of indicators I_{mr1}, I_{mr3} and I_{mc}. The ratio of indicator I_{mc1} in overvoltage condition to its value in normal condition is proportional to the overvoltage magnitude. Therefore it can be used as a good criterion for identification of overvoltage at leakage current measurement moment.
- Third harmonic of resistive current indicator (I_{mr3}) is sensitive to the presence of third harmonic of

voltage while the presence of third harmonic of voltage has the least effect on I_{mc1} and I_{mr1}. The third harmonic of resistive current (I_{mr3}) is greater than fundamental harmonic (I_{mr1}) in the presence of third harmonic in applied voltage.

- I_{mr1} and I_{mr3} in aged metal oxide surge arrester are greater when compared to the corresponding values in un-aged while I_{mc1} has a little change. So the observation and comparison of such variation in these indicators with their values in normal operating condition can be used for realizing aged surge arresters.

References

[1] Y. C. Kang, B. E. Lee, T. Y. Zheng and Y. H. Kim, "Protection, faulted phase and winding identification for the three-winding transformer using the increments of flux linkages", *Generation, Transmission and Distribution, IET*, Vol. 4, No. 9, pp. 1060-1068, 2010.

[2] S. Jiale, Z. Jiao, G. Song and X. Kang, "Algorithm to identify the excitation inductance of power transformer with wye-delta connection", *IET Electric Power Applications,* Vol. 3, No. 1, pp. 1-7, 2009.

[3] M. Khodsuz and M. Mirzaie, "Analysis of grading ring design parameters and heat sink numbers effect on voltage distribution and leakage current in metal oxide surge arrester", *Iranian Journal of Electrical and Electronic Engineering*, Vol. 10, No. 2, pp. 152-158, 2014.

[4] V. Behjat, A. Vahedi, A. Setayeshmehr and et al, "Sweep frequency response analysis for diagnosis of low level short circuit faults on the windings of power transformers: An experimental study", *International Journal of Electrical Power and Energy Systems*, Vol. 26, No. 4, pp. 78-90, 2012.

[5] A. Contin, G. Rabach, J. Borghetto and et al, "Frequency-response analysis of power transformers by means of fuzzy tools", *IEEE Transactions on Dielectrics and Electrical Insulation*, Vol. 18, No. 6, pp. 900-909, 2011.

[6] A. Bakar, H. Illias, M. Othman and H. Mokhlis, "Identification of failure root causes using condition based monitoring data on 33kV switchgear", *International Journal of Electrical Power and Energy Systems*, Vol. 47, No. 1, pp. 305–312, 2013.

[7] C. A. Christodouloua, L. Ekonomoub, G. P. Fotis and et al, "Assessment of surge arrester failure rate and application studies in Hellenic high voltage transmission lines", *Electric Power Systems Research*, Vol. 83, No. 11, pp. 176-83, 2010.

[8] S. Shirakawa, F. Endo, H. Kitajima and et al, "Maintenance of surge arrester by a portable arrester leakage current detector", *IEEE Transaction on Power Delivery*, Vol. 3, No. 3, pp. 998–1003, 1988.

[9] J. Lundquist, L. Stenstrom, A. Schei and B. Hansen, "New method for measurement of the resistive leakage current of metal-oxide surge arresters in service", *IEEE Transaction on Power Delivery*, Vol. 4, No. 5, pp. 1811–1822, 1990.

[10] L. T. Coffeen and J. E McBride, "High voltage ac resistive current measurements using a computer based digital watts technique", *IEEE Transaction on Power Delivery*, Vol. 4, No. 6, pp. 550–556, 1991.

[11] Z. Xu, L. Zhao, A. Ding and F. Lu, "A Current Orthogonality Method to Extract Resistive Leakage Current of MOSA", *IEEE Transaction on Power Delivery*, Vol. 28, No. 1, pp. 93-101, 2013.

[12] C. A. Christodoulou, M. V. Avgerinos, L. Ekonomou and et al, "Measurement of the resistive leakage current in surge arresters under artificial rain test and impulse voltage subjection", *IET Science, Measurement & Tech.,* Vol. 3, No. 3, pp. 256-262, 2009.

[13] C. A. L. Almeida, A. P. Braga, S. Nascimento and V. Paiva, "Intelligent Thermographic Diagnostic Applied to Surge Arresters. A New Approach", *IEEE Transaction on Power Delivery*, Vol. 3, No. 1, pp.751-757, 2009.

[14] G. R. S. Lira, E. G. Costa and C. W. D. Almeida, "Self-organizing maps applied to monitoring and diagnosis of ZnO surge arresters", *Transmission and Distribution Conference and Exposition. Latin America (T&D-LA)*, pp. 659-664, 2010.

[15] K. L Wong, "Electromagnetic emission based monitoring technique for polymer ZnO surge arresters", *IEEE Transaction on Dielectrics and Electrical Insulation*, Vol. 1, No, 13, pp.181-190, 2006.

[16] J. Xu, A. Kubis, K. Zhou, Zh. Ye and L. Lou, "Electromagnetic field and thermal distribution optimization in shell-type traction transformers", *IET Electric Power Applications,* Vol. 7, No. 8, pp. 627-632, 2013.

[17] Z. N. Stojanovic and Z. M Stojkovic, "Evaluation of MOSA condition using leakage current method", *International Journal of Electrical Power and Energy Systems*, Vol. 52, No. 1, pp. 87-95, 2013.

[18] M. Khodsuz, M. Mirzaie and S. M. Seyyedbarzegar, "Metal oxide surge arrester condition monitoring based on analysis of leakage current components", *International Journal of Electrical Power and Energy System*s, Vol. 66, No. 1, pp. 188-193, 2015.

[19] B. H. Lee and S. M. Kang, "A new on-line leakage current monitoring system of ZnO surge arresters", *Article Materials Science and Engineering. B*, Vol. 119, No. 1, pp. 13-18, 2005.

[20] H. Zhu and M. R Raghuveer, "Influence of representation model and voltage harmonics on metal oxide surge arrester diagnostics", *IEEE Transaction on Power Delivery*, Vol. 4, No. 14, pp. 599-603, 2001.

[21] H. Zhu and M. R. Raghuveer, "Influence of harmonics in system voltage on metal oxide surge arrester diagnostics", *Conference on electrical insulation and dielectric phenomena. Austin, USA*, pp. 17-20, 1999.

[22] C. Cortes and V. Vapnik, "Support vector Networks, Machine Learn", *Machine Learning*, Vol. 20, No. 3, pp. 273–295, 1995.

[23] G. Lv, H. Cheng, H. Zhai and L. Dong, "Fault diagnosis of power transformer based on multilayer SVM classifier", *Electric Power Systems Research*, Vol. 75, No. 1, pp. 9-15, 2005.

Masume khodsuz was born in Sari, Iran in 1985. She received the B.Sc. and M.Sc. degree in power engineering both from Mazandaran University of Technology in 2007 and 2010, respectively and Ph.D. Degree in power Engineering from the Babol University of technology in high voltage engineering in 2015. Her research interests are electric field and magnetic field analysis, high-voltage engineering and also power quality.

Mohammad Mirzaie was born in Ghaem-Shahr, Iran in 1975. Obtained B.Sc. and M.Sc. Degrees in Electrical Engineering from University of Shahid Chamran, Ahvaz, Iran and Iran University of Science and Technology, Tehran, Iran in 1997 and 2000 respectively and Ph.D. Degree in Electrical Engineering from the Iran University of Science and Technology in 2007. He worked as an Assistant Professor in the electrical and computer engineering department of Babol University of technology from 2007. His research interests include life management of high voltage equipments, high voltage engineering, intelligence networks for internal faults assessment in equipment and studying of insulation systems in transformers, cables, generators, breakers, insulators, electrical motors.